JACS
JOURNAL OF THE AMERICAN CHEMICAL SOCIETY
pubs.acs.org/JACS
Article

Probing the Origins of the Disorder-to-Order Transition of a Modified Cholesterol in Ternary Lipid Bilayers

Ayan Majumder, Yuanqing Gu, Yi-Chen Chen, Xingda An, Björn M. Reinhard, and John E. Straub*

Cite This: https://doi.org/10.1021/jacs.4c09495
Read Online

ABSTRACT: In a recent study, spectroscopic observations of modified cholesterol in both lipid-coated nanoparticles and liposomes provided evidence for a disorder-to-order orientational transition with increasing temperature. Below a critical temperature, in a membrane composed of modified cholesterol, saturated (DPPC) lipid, and anionic (DOPS) lipid, a roughly equal population of head-out and head-in conformations was observed. Surprisingly, as temperature was increased the modified cholesterol presented an abrupt transition to a population of all head-in orientations. Additionally, when saturated DPPC lipids were replaced by unsaturated DOPC the disorder-to-order transition was eliminated. To gain insight into this curious transition, we use all-atom molecular dynamics simulations to characterize the structure and fluctuations of lipid bilayers composed of saturated and unsaturated lipids, in the presence of normal and modified cholesterol. Free energy differences between head-out and head-in conformations are computed as a function of varying lipid membrane composition for normal and modified cholesterol. In bilayers primarily composed of DPPC, the orientation of modified cholesterol is observed to depend sensitively on the orientation of the surrounding normal or modified cholesterol molecules, suggesting cooperative Ising-like interactions favoring an ordered state. In bilayers primarily composed of DOPC, spontaneous flip-flop of modified cholesterol is observed, consistent with the measured small free energy barrier separating the head-in and head-out orientations. This combined experimental and computational study effectively characterizes the orientational dimorphism and provides novel insight into the fundamental nature of cholesterol interactions in membrane.

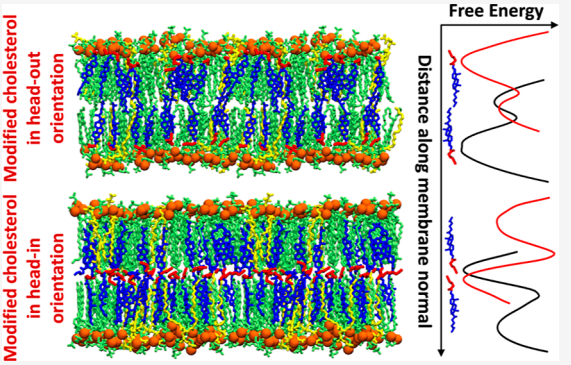

INTRODUCTION

Cholesterol is the most abundant molecule in mammalian plasma membranes with typical compositions varying from 30 to 40 mol %.[1,2] It is a polycyclic and amphiphilic molecule with a flat asymmetric structure.[3,4] Martin and Yagel showed that cholesterols form face-to-face dimers stabilized by van der Waals interactions using an X-ray diffraction study of lipid-solvated cholesterols.[5] The hydroxyl group of cholesterol, defined as the "head" group, interacts with the polar moiety of lipids, proteins, and interfacial water molecules through hydrogen bonding.[3,6] Previous studies have shown that cholesterol influences the rigidity and permeability of the membrane and mediates the formation of the ordered phase in a lipid bilayer.[7,8] In addition, cholesterol facilitates phase separation within the lipid bilayer and the formation of so-called lipid rafts by preferentially interacting with saturated lipids.[9,10] Cholesterol is also known to interact with membrane proteins and is suspected to play a role in the onset of Parkinson's and Alzheimer's diseases.[11,12]

Membrane cholesterol is known to modulate lipid phase separation and membrane fluidity. As a function of temperature, lipid membranes may present a cooperative melting transition between a solid-like phase, predominant at low temperatures, and a fluid phase, predominant at high temperatures. The addition of cholesterol acts to broaden the transition in temperature, increasing fluidity at lower temperatures, by fluidizing the solid phase, and decreasing fluidity at high temperatures, by ordering lipids. Overall, the effect is to shift and broaden the transition in fluidity with increasing temperature.

Uneven lipid distribution across different leaflets of a lipid bilayer has significant relevance in membrane biology.[13−15] The uneven distribution of lipids in membrane bilayers is maintained by the trans-bilayer movement of phospholipids, facilitated by the ATP-mediated flipase and flopase.[13−16] The flip-flop of phospholipids occurs on a longer physiological time scale (∼hours),[17,18] whereas the spontaneous flip-flop of cholesterol occurs much faster.[19−22] Because of the smaller hydrophilic group present in the cholesterol, flip-flop occurs without the presence of ATP. The fast intrabilayer flip-flop of

Received: July 12, 2024
Revised: September 13, 2024
Accepted: September 16, 2024

https://doi.org/10.1021/jacs.4c09495
J. Am. Chem. Soc. XXXX, XXX, XXX−XXX

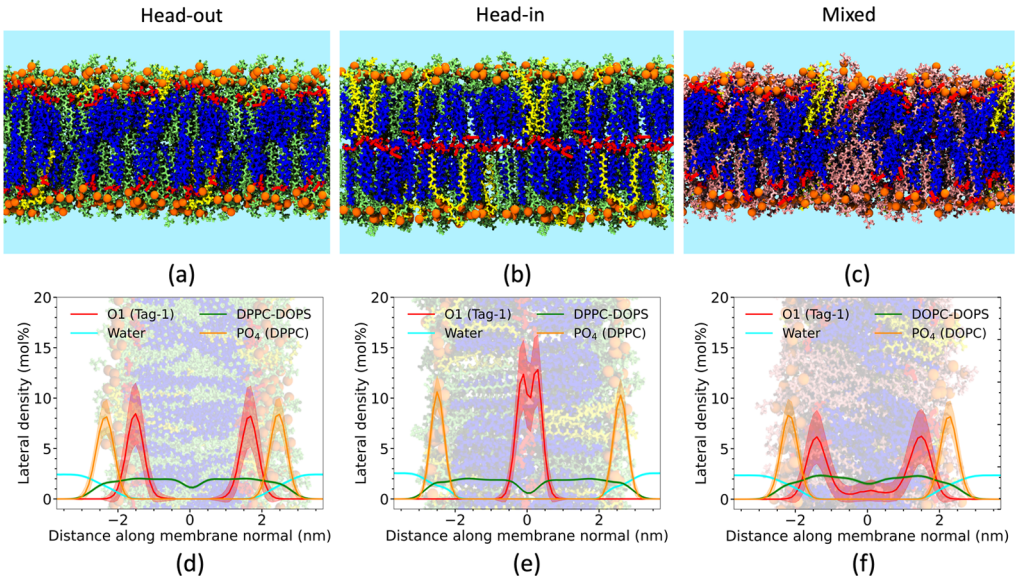

Figure 1. Pictorial representation and lateral density profiles of lipid bilayers composed of DPPC (green), DOPS (yellow), and Tag-1 (blue) in the (a,d) head-out and (b,e) head-in orientations, and (c,f) lipid bilayer composed of DOPC (pink), DOPS (yellow), and Tag-1 (blue) in a mixed orientational state. Head group of Tag-1 is represented in red. Traces represent the density distributions of Tag-1 O1 atom (red), water (cyan), lipid (green), and lipid headgroup (orange), respectively. The midpoint along the membrane normal was set to zero to guide the comparison. Tag-1 molecules were found to be stable in both head-out and head-in orientations in DPPC, whereas a mixed orientational state of Tag-1 was observed in DOPC.

cholesterol plays a crucial role in relaxing membrane stress and modulating lipid distribution.[21,23]

The significance of the uneven distribution of cholesterols remains largely unknown. The interleaflet motion of cholesterols in lipid bilayers has been extensively studied experimentally[20,21,24,25] and computationally.[22,26−30] The time scale obtained from different studies varies from submilliseconds to minutes. Free energy calculations have been performed to understand the cholesterol flip-flop process and different conformations of cholesterol were characterized. It has been shown that cholesterol flip-flop occurs significantly faster in a bilayer composed of unsaturated lipids[26,31] or a bilayer containing low cholesterol concentrations.[22,30] These findings suggest that the membrane environment around cholesterol has a significant influence on determining the flip-flop energetics.

Modified forms of cholesterol have been developed to exploit the central role of cholesterol in the context of biochemistry and biomaterials. In our previous work, we modified cholesterol to create the Tag-1 molecule by substituting the hydroxyl group with an ester linkage to a 5-hexyne chain. The substitution is equivalent with replacing a polar methanol moiety with methyl-5-hexynoate containing a terminal alkyne group (Supporting Information Figure 1).[32] The added terminal alkyne group provides a distinct Raman frequency characteristic of the local chemical environments. A Tag-1 molecule can assume the head-out orientation, with the terminal alkyne group pointing toward the water, or the head-in orientation, with the terminal alkyne group pointing toward the middle of the membrane bilayer. Through analysis of the modified lipids and application of the click chemistry, we showed that the Tag-1 molecule coexists in both head-out and head-in orientations at room temperature in liposomes or lipid-coated noble metal nanoparticles (L-NPs). Additionally, we observed an all-or-none phase transition to an all head-in state in a bilayer composed of saturated lipids at high temperatures. The transition appears surprising in that the disordered state is dominant at low temperatures while the ordered state is observed at high temperatures. We proposed that the hydrogen bonding network between lipid and interfacial water plays a crucial role in determining the relative probability of head-out and head-in orientations of Tag-1 at higher temperatures.[32] However, our understanding of the thermodynamics of different orientations of Tag-1 at room temperature remains incomplete.

In this work, we employed all-atom simulations of membrane bilayers containing Tag-1 in the presence of saturated lipid (DPPC) or unsaturated lipid (DOPC) to characterize the thermodynamic driving forces controlling the disorder-to-order transition of Tag-1 in lipid bilayers. The structural ensembles of Tag-1 are characterized by calculating the density distributions and Crick angle. Umbrella sampling simulations were used to understand the underlying mechanism of Tag-1 flip-flop in saturated and unsaturated lipid environments. The results obtained from the simulations provide insight into the nature of the disorder-to-order transition.

RESULTS AND ANALYSIS

Characterizing the Membrane Structure with Tag-1 in Head-in, Head-out, and Mixed States. We conducted all-atom simulations of lipid bilayers composed of 55 mol % DPPC/DOPC, 5 mol % DOPS, and 40 mol % Tag-1 (see methods and Supporting Information Figure 1) at room temperature. To characterize the orientational preference of Tag-1 molecules, we performed separate simulations starting from Tag-1 in either all head-out or all head-in orientations in membrane bilayers containing either DPPC or DOPC. The final configuration of bilayers obtained from these simulations is shown in Figure 1. Density distributions of lipid bilayers containing varying lipid components obtained from simulations are shown in Figure 1. In a membrane bilayer

https://doi.org/10.1021/jacs.4c09495
J. Am. Chem. Soc. XXXX, XXX, XXX−XXX

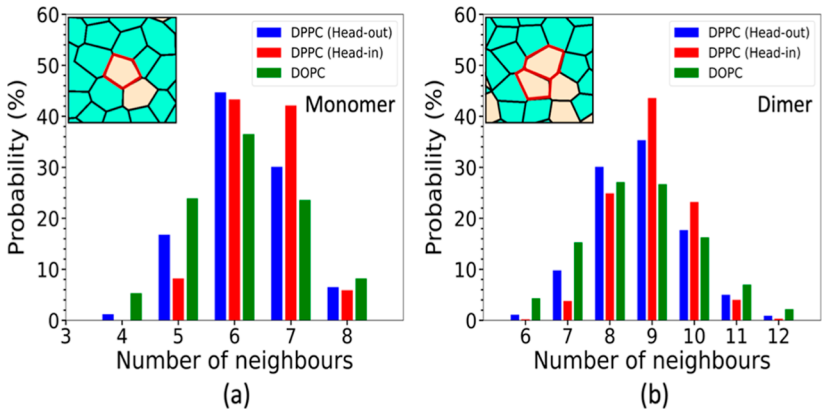

Figure 2. Distributions of NNs (lipid tail or Tag-1) for (a) Tag-1 monomers and (b) Tag-1 dimers obtained from simulations of Tag-1 in the head-out orientation in DPPC, the head-in orientation in DPPC, and in a mixed orientational state in DOPC. The distributions obtained are consistent with previous studies of normal cholesterol.[5,37,38]

containing DPPC, starting from either all head-out or all head-in orientations of Tag-1, we observed distinct peaks due to the orientation of the alkyne group toward the membrane−water interface or the middle of the membrane, respectively. This suggests that both orientations of Tag-1 are thermodynamically relevant in a lipid bilayer at room temperature. Whereas in a membrane bilayer containing DOPC, we observed spontaneous flip-flop of Tag-1 molecules in unbiased simulation. Starting from either an all head-out or all head-in orientation of Tag-1, we obtained a mixed state of head-out and head-in orientations (Figure 1f).

Several computational studies on membrane bilayers containing 40 mol % cholesterol in DPPC or DOPC have also predicted the formation of a liquid-ordered phase in DPPC and a liquid-disordered phase in DOPC at room temperature.[33−35] By analyzing the liquid crystal order parameter (P_2) values of DPPC, we previously showed that Tag-1 behaves similarly to normal cholesterol and forms a liquid-ordered phase in a membrane composed of 55 mol % DPPC, 5 mol % DOPS, and 40 mol % Tag-1 in head-out or head-in orientations. The average P_2 value of lipid tails obtained from simulations of all membrane bilayers studied is shown in Supporting Information Table 1. The results show that the membrane composed of 40 mol % Tag-1, 55 mol % DOPC, and 5 mol % DOPS forms a liquid-disordered phase.

At room temperature, in an experimentally prepared membrane system without any external bias in membrane preparation, we expect an equal population of Tag-1 in head-in and head-out orientations. Although spontaneous flip-flop of Tag-1 is not possible on the time scale of our simulations due to a high energy barrier in the membrane consisting of DPPC, both head-in and head-out orientations represent thermodynamically stable states dependent on the orientations of the neighboring Tag-1 molecules. This assumption is supported by the experimental observation that two distinct peaks of equal intensity correspond to head-in and head-out orientations of Tag-1.[32] The spontaneous flip-flop of Tag-1 in a bilayer containing DOPC explains the experimental observation of a doublet peak characterizing a mixed state of head-out and head-in orientations (Supporting Information Figure 2).

For membranes primarily composed of DPPC, when the temperature of the system was increased above 64 °C we observed a surprising doublet-to-singlet transition in the Raman spectra that we interpret to be a transition in the orientational distribution of Tag-1 from a mixed state, of roughly equal populations of head-in and head-out orientations, to an ordered head-in state. However, this doublet-to-singlet transition was absent in systems primarily composed of DOPC over all temperatures studied. The transition was also absent in systems primarily composed of DPPC when the monovalent salt concentration was increased to 300 mM.

These results beg the question of whether the mixed orientational state is an equilibrium state of those systems primarily composed of DPPC. Experiments were performed in which the system at elevated temperature in an all head-in state was cooled to room temperature. We observed a singlet-to-doublet transition in the Raman spectra that we interpret to be a return to the mixed orientational state. This demonstrates that the mixed state, characterized by roughly equal populations of head-in and head-out orientations of Tag-1, is the equilibrium state of the system at room temperature. Interestingly, this transition is observed to be very slow with measurable conversion of the population appearing after 4 weeks and complete transition to the equilibrium mixed state occurring after 6 weeks (Supporting Information Figure 3).

Greatest Number of Nearest Neighbors for Tag-1 is Observed for the Head-in State. Voronoi tessellation has been extensively used to calculate the area of the lipids or to understand the spatial lipid distribution in multicomponent lipid bilayers.[9,36] Engelman et al. studied a binary mixture of dipalmitoyl lecithin and cholesterol using wide-angle X-ray diffraction to show that the cholesterol monomers are surrounded by seven lipid tails.[37] Martin and Yeagle showed that cholesterol dimers were surrounded by nine lipid tails, while cholesterol monomers were surrounded by five lipid tails.[5] In a computational study using the CHARMM36 force field, Straub and co-workers also predicted six/seven nearest neighbors (NN) of cholesterol in binary or ternary lipid mixtures containing 10−20 mol % cholesterol.[38]

We performed Voronoi tessellation to understand the spatial distribution of lipids and Tag-1 in the membrane. Each polygon in the tessellation represents one lipid tail or one Tag-1 molecule. The number of NN of a Tag-1 was calculated by counting the edges of the Voronoi polygon corresponding to that Tag-1 molecule. The NN distributions of Tag-1 monomers and dimers obtained from the simulations of Tag-1 in different orientational states in a lipid bilayer are shown in Figure 2.

https://doi.org/10.1021/jacs.4c09495
J. Am. Chem. Soc. XXXX, XXX, XXX−XXX

The results show that Tag-1 monomers have similar NN distributions in a membrane bilayer containing DPPC or DOPC. The NN distributions of Tag-1 monomers and dimers peaked at six and nine NNs, respectively, in line with previous studies of normal cholesterol. However, Figure 2 shows that the Tag-1 monomers in the head-in orientation show a higher number of contacts with their neighbor lipid molecules compared to the Tag-1 monomers in the head-out orientation. This indicates that in bilayers containing DPPC and Tag-1 monomers, the bilayer is significantly more compact with Tag-1 in the head-in orientation as opposed to the head-out orientation. The NN distributions of Tag-1 monomers when considering only the nearest Tag-1 and only lipid tails are shown in Supporting Information Figure 4.

Cholesterol and Tag-1 Dimers Preferentially form Face-to-Face Orientations. Martin and Yeagle predicted the formation of face-to-face cholesterol dimers in lipid bilayers facilitated by the interaction of their α-faces, which was predicted to be stabilized by the van der Waals interactions through the closer contacts of the sterol moieties.[5] Previous computational study of phospholipid bilayers containing 20 mol % cholesterol also showed a predominant population of $\alpha\alpha$ dimers with minor populations of $\beta\beta$- or t-dimers (Supporting Information Figure 5).[38] The Crick angle distributions of Tag-1 dimers obtained from the simulation of Tag-1 in all head-out or all head-in orientations in DPPC are shown in Figure 3.

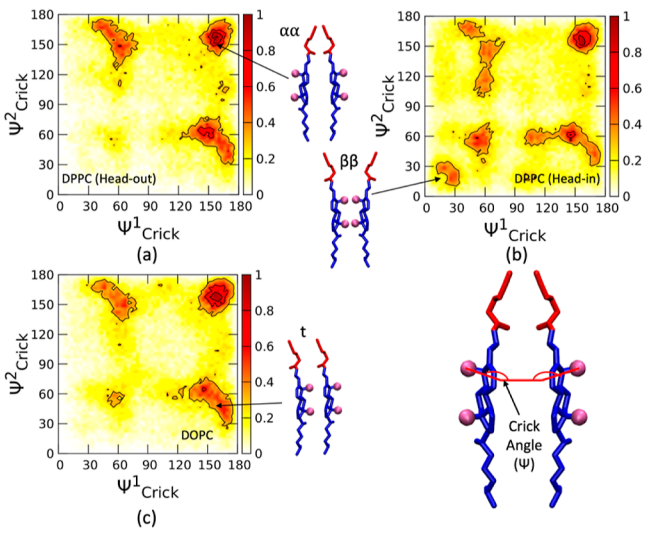

Figure 3. Crick angle distributions of Tag-1 dimers obtained from simulations of Tag-1 in the (a) head-out orientation in DPPC, (b) head-in orientation in DPPC, and (c) in a mixed orientational state in DOPC. Crick angle distribution of Tag-1 dimers in DOPC was calculated when both Tag-1 molecules are in same orientation. The distributions show that Tag-1 primarily forms $\alpha\alpha$- and t-dimeric conformations.

The distributions show that the Tag-1 dimers are stabilized by the interaction facilitated by the α-face of the sterol rings to form $\alpha\alpha$- or t-dimers. The ratio of $\alpha\alpha/\beta\beta$/t dimers in membrane bilayer containing Tag-1 in head-out and head-in orientations in DPPC was found to be 1.0:0.07:1.17 and 1.0:0.64:0.99, respectively. We also calculated the Crick angle distribution of Tag-1 dimers in DOPC when both Tag-1 molecules are in like orientation (both Tag-1 in head-out or head-in). A similar pattern was observed where Tag-1 dimers primarily form $\alpha\alpha$- or t-conformations with the ratio of $\alpha\alpha/\beta\beta$/t dimers to be 1.0:0.09:0.91 (Figure 3c).

To better understand the interaction of Tag-1 with other lipid components, we calculated the density distribution of lipid components around Tag-1 by aligning the reference vector (C17−C18) of Tag-1 along the positive x-axis. The negative x-direction of the density distribution represents the α-face of Tag-1. The population density of Tag-1 around a central Tag-1 is shown in Figure 4 and the population density of lipids around Tag-1 is shown in Supporting Information Figure 6.

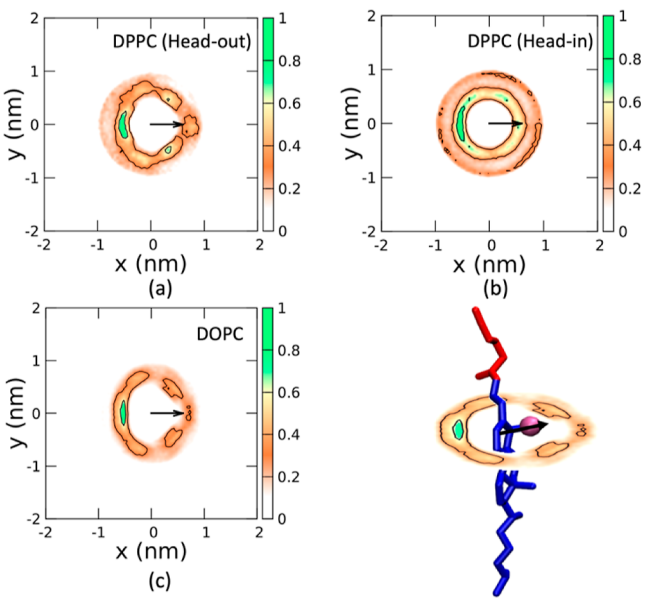

Figure 4. Population density in the xy-plane of Tag-1 molecules around a central Tag-1 molecule obtained from simulations of Tag-1 in the (a) head-out orientation in DPPC, (b) head-in orientation in DPPC, and (c) in a mixed state of head-out and head-in orientations in DOPC. In a membrane containing DOPC, density distribution around a Tag-1 was calculated when neighboring Tag-1 molecules assumes a like orientation. Pictorial representation of Tag-1 and the reference vector (C17−C18) oriented along the positive x-axis is represented by a black arrow. The distributions show that the Tag-1 primarily interacts with the other Tag-1 molecules through the α-face.

The binding of lipids is found to be isotropic around Tag-1 showing no preferential binding orientation (Supporting Information Figure 6). In contrast, Tag-1 molecules were found to interact with other Tag-1 molecules through the α-face in both ordered and disordered lipid bilayers, as expected from Crick-angle distributions. This specific interaction pattern of Tag-1 interacting through the α-face was not observed when Tag-1 dimers assumed antiparallel orientations (Supporting Information Figure 7).

Free Energy of Tag-1 Strongly Favors Alignment with Neighboring Tag-1 Molecules. To characterize the energy barrier separating two different orientations of a Tag-1 molecule, we calculated the potential of mean force (PMF) along a collective variable defined by the distance between the headgroup (O1 atom) of Tag-1 and the midpoint of the lipid bilayer. The results are shown in Figure 5. In a membrane containing DPPC and Tag-1, the PMFs represent the transition of a Tag-1 from head-out to head-in orientation when all other Tag-1 molecules are either in head-out orientation (Figure 5a) or head-in orientation (Figure 5b),

https://doi.org/10.1021/jacs.4c09495
J. Am. Chem. Soc. XXXX, XXX, XXX−XXX

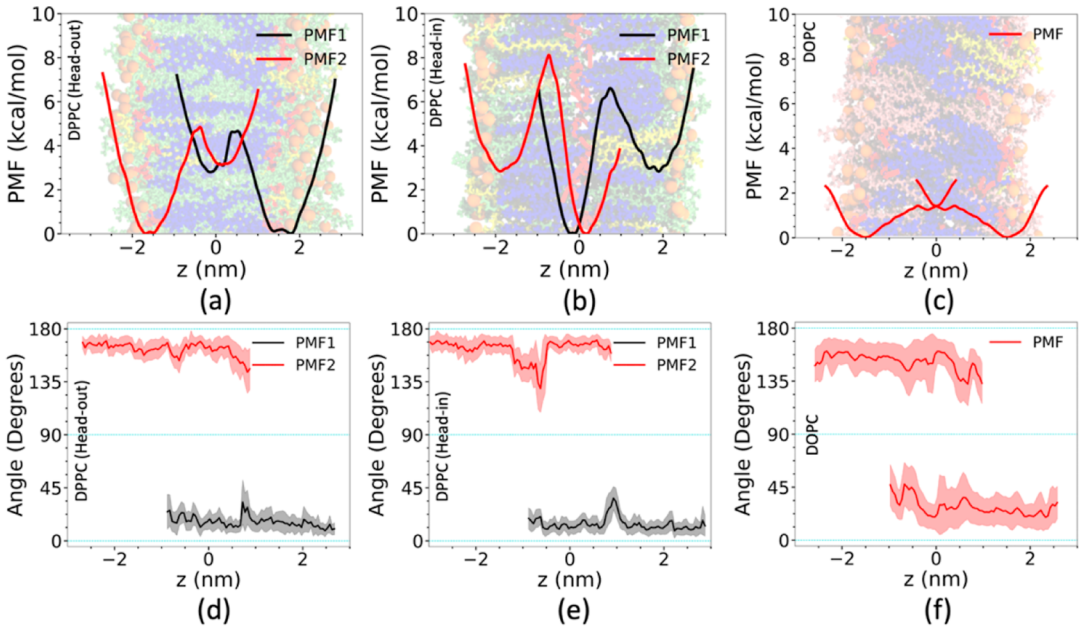

Figure 5. (Upper) PMF for the head-in to head-out orientational change of the Tag-1 molecule and (lower) the angular distributions characterizing the orientations of Tag-1 relative to the *z*-direction normal to the membrane obtained from simulations of Tag-1 in (left; a,d) the head-out orientation in DPPC, (center; b,e) head-in orientation in DPPC, and (right; c,f) in a mixed state of head-out and head-in orientations in DOPC. PMFs and angle distributions obtained in DOPC were computed assuming symmetry in the leaflets to compare with the PMFs obtained in DPPC. A cooperative effect, stabilizing the like orientation of Tag-1, was observed in the ordered membrane consisting of DPPC.

respectively. The PMFs suggest that both orientations of Tag-1 are stable in DPPC at 303 K. The most stable orientation of Tag-1 depends on the relative orientations of surrounding Tag-1 molecules. To explore the role of interactions mediated by the sterol rings and alkyne moiety of Tag-1, we calculated the PMF characterizing the head-in to head-out orientational transition of a Tag-1 molecule in the presence of normal cholesterol (Supporting Information Figure 8). The resulting PMFs are similar to those found for membrane composed of DPPC and Tag-1 suggesting that the cholesterol/Tag-1 interactions are similar to Tag-1/Tag-1 interactions. As such, we conclude that the favorable interactions are primarily mediated by interactions mediated by the sterol rings.

When the nearby Tag-1 molecules are in the head-in orientation, the head-in orientation of Tag-1 is more stable than the head-out orientation by approximately 3 kcal/mol. Similarly, when the nearby Tag-1 molecules are in the head-out orientation, the head-out orientation of Tag-1 is more stable than the head-in orientation by approximately 3 kcal/mol. As such, there is a substantial energetic bias toward an ordered state of all head-out or all head-in state. Notably, the free energy barriers $\Delta G^{\neq}$ for transitions between head-out from head-in conformations in a bilayer containing all other Tag-1 molecules in a head-out orientation in DPPC are found to be $\Delta G^{\neq}_{\text{head-out}\rightarrow\text{head-in}}$ = 5 kcal/mol and $\Delta G^{\neq}_{\text{head-in}\rightarrow\text{head-out}}$ = 1.5 kcal/mol. These barriers are noticeably different from those observed for transitions between head-out from head-in conformations in a bilayer containing all other Tag-1 molecules in head-in orientations in DPPC, which are found to be $\Delta G^{\neq}_{\text{head-out}\rightarrow\text{head-in}}$ = 4.5 kcal/mol and $\Delta G^{\neq}_{\text{head-in}\rightarrow\text{head-out}}$ = 7 kcal/mol.

In a membrane containing DOPC and Tag-1, the Tag-1 molecules maintain a mixed orientational state, with no strong preference for either orientation. Therefore, a random Tag-1 molecule is selected and dragged from a head-out to a head-in orientation while the neighboring Tag-1 molecules remain in a mixed orientational state. PMF predicts that the energetic difference between the two orientational states of Tag-1 is relatively small in DOPC, about 1.3 kcal/mol (Figure 5c). There is only a small energy barrier to flipping between head-out and head-in orientations. This demonstrates that both head-out and head-in orientations of Tag-1 are kinetically accessible. This observation is in line with the experimental results that the Tag-1 molecules were found in the mixed orientational state in a bilayer composed of unsaturated lipids.

Additionally, we determined the angular distribution between the director vector of the biased Tag-1 defined by the center-of-mass through the headgroup (O1 atom) and the membrane normal, where the angles of 0 and 180° denote a Tag-1 structure parallel to the membrane normal and 90° denotes a Tag-1 structure perpendicular to the membrane normal (Supporting Information Figure 9). Figure 5 shows the angular distribution characterizing the orientation of Tag-1 relative to the membrane normal along the collective variable defining the flip-flop process. Previous computational studies on normal cholesterol and modified forms of cholesterol predicted both parallel and perpendicular orientations of the molecule with respect to the membrane normal.[26,39] In the liquid-ordered phase of the membrane containing DPPC, we observed only small orientational fluctuations of the biased Tag-1 molecule which prefers a parallel orientation. In contrast, a frequent transition between parallel and perpendicular orientations of Tag-1 was noted in the liquid-disordered phase of the membrane containing DOPC.

Assessing Membrane Fluidity Using C-Laurdan Generalized Polarization Measurements. Spectroscopic analysis of C-Laurdan has been widely used to assess the fluidity of lipid bilayers.[40,41] Generalized polarization (GP) and fluorescence anisotropy analyses have been shown to effectively capture membrane phase transitions.[42] The GP

https://doi.org/10.1021/jacs.4c09495
J. Am. Chem. Soc. XXXX, XXX, XXX−XXX

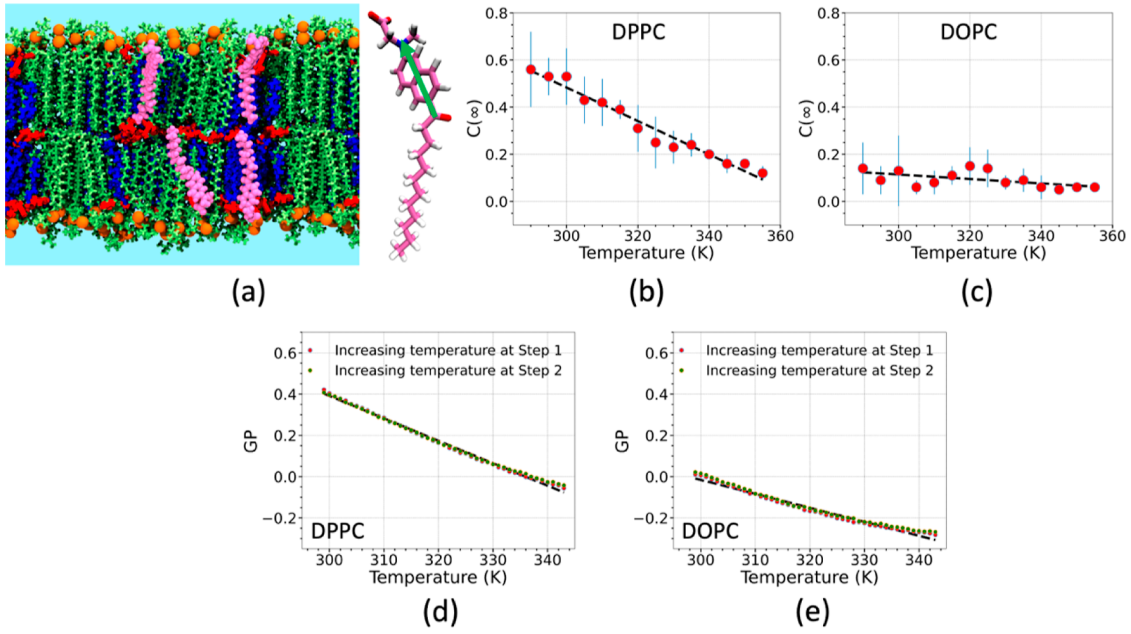

Figure 6. (a) Pictorial representation of the membrane bilayer containing C-Laurdan (mauve) and the dipole vector of C-Laurdan represented by a green arrow.[40] $C(\infty)$ value of C-Laurdan obtained from the simulations of membrane bilayer containing (b) DPPC or (c) DOPC over a broad range of temperatures. The experimental GP value of C-Laurdan in a liposome containing (d) DPPC or (e) DOPC over a broad range of temperatures.

analysis is sensitive to changes in the polarity of the membrane environment. Fluorescence anisotropy analysis captures orientational fluctuations of the fluorescent probe to detect changes in the membrane order. To study membrane fluidity at different temperatures, we simulated a lipid bilayer, composed of C-Laurdan, DOPS, Tag-1, and DPPC/DOPC, varying the temperature from 295 to 355 K.

Lipari and Szabo[43] and Ikegami et al.[44] proposed theories relating the time-dependent fluorescence anisotropy $r(t)$ to the rotational correlation function $C(t)$ of the fluorescent probe. It was shown that $r(t)/r(0) = C(t) = \langle P_2(\vec{\mu}(0)\cdot\vec{\mu}(t))\rangle$ where μ is the dipole vector, the initial time value of the fluorescence anisotropy is $r(0) = \frac{2}{5}P_2(\cos\delta)$, and δ is the angle between the absorption and emission dipole vectors of the fluorescent probe. The second-order Legendre polynomial $P_2(x) = (3x^2 - 1)/2$ describes the orientational distribution of the fluorescent probe. It is often assumed the $C(t)$ decays exponentially in time as $C(t) = C(\infty) + (1 - C(\infty))e^{-\beta t}$. The infinite time limit value $C(\infty)$ obtained from simulations at varying temperatures is shown in Figure 6. The observed time-dependence of the computed $C(t)$ in bilayers containing DPPC and DOPC is shown in Supporting Information Figures 10 and 11, respectively.

Harris et al.[42] studied the phase transition of the membrane bilayer over a range of cholesterol concentrations by calculating the GP and fluorescence anisotropy of Laurdan. They demonstrated that at low cholesterol concentrations the phase transition of the membrane can be characterized by the sigmoidal pattern of the GP and fluorescence anisotropy values at the transition temperature. However, at high cholesterol concentrations the GP and fluorescence anisotropy values are observed to decrease gradually and present no abrupt transition.

We performed experimental studies of membrane fluidity through an analysis of C-Laurdan fluorescence, both in membranes predominantly composed of DPPC and those predominantly composed of DOPC. The GP value of C-Laurdan as a function of temperature was measured in two steps. (1) After preparing the liposome at room temperature the GP value was measured by heating the system to 343 K. (2) The liposome was then cooled to room temperature and reheated to 343 K to measure the GP value at varying temperatures. The results for the measured GP values in two steps are consistent showing no evidence of hysteresis (Figure 6). Reinhard and co-workers have analyzed the GP values of C-Laurdan to effectively characterize the phase transition of membrane containing DPPC and cholesterol concentrations below 20 mol % characterized by the sigmoidal pattern of the GP values. While in a membrane consisting of 40 mol % cholesterol, the phase transition is substantially broadened and no longer detectable.[45]

Figure 6 shows that the fluidity of the membrane bilayer containing DPPC gradually decreases with an increase in temperature absent an abrupt phase transition. The membrane bilayer containing DOPC remains in the liquid-disordered phase at all temperatures studied. Our simulation and experimental results suggest that for the lipid bilayers formed of 40 mol % CHOL or Tag-1, there is no measurable transition in membrane fluidity of phase as a function of temperature over the temperature range studied.

DISCUSSION

No Lipid Phase Transition Observed over the Range of Temperatures Studied. Our simulation and experimental results provide evidence that over the range of temperatures studied in experiment, the lipid mixtures remain in a fluid phase. There is no evidence of a phase transition that could drive the observed disorder-to-order transition observed in systems having 40 mol % Tag-1. This conclusion is supported by prior experimental studies of the phase diagram of membrane bilayers containing DPPC, DOPC, and cholesterol.

https://doi.org/10.1021/jacs.4c09495
J. Am. Chem. Soc. XXXX, XXX, XXX−XXX

Chiang et al. studied a binary mixture of DPPC and cholesterol at varying cholesterol concentrations and temperatures using the 2D electron−electron double resonance method to show that a membrane composed of 60 mol % DPPC and 40 mol % cholesterol forms a liquid-ordered phase at room temperature.[46] Vist and Davis also reported the formation of a β-phase in a membrane (liquid-ordered) at room temperature containing cholesterol concentrations above 22 mol %.[47] Nyholm et al. showed that the membrane composed of 60 mol % DOPC and 40 mol % cholesterol forms a liquid-disordered phase by measuring the fluorescence lifetime of *trans*-parinaric acid.[48] Konyakhina et al. also reported the formation of a liquid-disordered phase by studying similar membrane compositions.[49] We conclude that a phase transition in the lipid bilayer is not responsible for the observed transition at high temperatures to an ordered state of head-in Tag-1 in LNP and liposomes composed of 55:40:5 DPPC/Tag-1/DOPS.

Transition to Head-in State of Tag-1 is Favored by Sterol−Sterol Interactions and Hydrogen Bonding. Our computational studies have demonstrated that the preferred orientation of Tag-1 is strongly dependent on the orientations of the surrounding Tag-1 molecules. Our evidence suggests that similarly orientated Tag-1 molecules, be it head-in or head-out, form favorable interactions between their sterol groups. It is also possible that the head-in and head-out orientations have differing interactions with the surrounding water. In our earlier work, we noted that with the Tag-1 in the head-out orientation, the alkyne group disrupts the hydrogen bond network formed by lipids head groups and water. More hydrogen bonds are formed between water and the lipid head groups with Tag-1 in the head-in orientation.

As was shown in our previous study[32] the transition from the head-out to head-in state of Tag-1 leads to a significant increase in DPPC lipid−water hydrogen bonding. As is apparent in Figure 1, in the head-in state the Tag-1 molecules are more deeply embedded in the lipid bilayer relative to the head-out state in which Tag-1 disrupts the network of hydrogen bonds between water and the DPPC lipid head groups. As such, the head-in state is enthalpically favored over the head-out state by a combination of increased water−lipid hydrogen bonding and more favorable sterol−sterol interactions.

Modeling the Tag-1 Disorder−Order Transition Using Ising-like Models. The simulations presented in this study demonstrate the importance of cooperative interactions between neighboring Tag-1 molecules that strongly favor alignment of the Tag-1 molecules into all head-out or all head-in states. However, in experiment only the disordered mixed state and ordered head-in states are observed. The computed free energy surfaces suggest similar stabilities for the all head-out and all head-in states. Moreover, that bias is observed even at room temperature where the mixed state is observed in experiment. This form of orientationally dependent interaction, that favors alignment of nearest-neighbor Tag-1 molecules, is reminiscent of cooperative transitions between disordered and ordered states, such as the ferromagnetic phase transition and the coil-to-helix transition.

Disorder-to-order transitions are commonly studied using an Ising-like model. For our system, we might use a 2D Ising-like model with nearest-neighbor interactions favoring the alignment of NN Tag-1 molecules. However, such a model predicts the disordered state to be dominant at high temperature and the ordered state to be observed at low temperature. In contrast, we observe the ordered head-in state to be dominant at high temperature. This suggests an important role for changes in enthalpy and entropy of the solvent, rather than the membrane alone, in determining the thermodynamically dominant state of the system.

Comparison with the Phenomenon of "Cold Denaturation" in Peptides and Proteins. A well-known biomolecular transition in which the disordered state is dominant at low temperatures is the phenomenon of cold denaturation. In cold denaturation, the unfolding temperatures are typically below 0 °C and the freezing point of water, and ice formation in the solvent plays a role destabilizing the folded state. In this study, the disorder to order transition occurs at high temperatures on the order of 60 °C. As such, the mechanism responsible for cold denaturation, which produces the disordered protein state at low temperature and ordered protein state at high temperature is not relevant to our study.

Nevertheless, there are significant changes in the properties of the water solvent over the range of temperatures studied. At 60 °C, water is less polar with a substantially smaller dielectric constant of 66.8 compared with 78.3 at 25 °C and 87.7 at 0 °C. This reflects a reduction of the induced dipole of water at higher temperatures with an associated weakening of hydrogen bonding. In our simulation models, we employ a fixed charge approximation that fails to capture changes in the polarization of water that underlies these changes. A polarizable water model could be used to assess the importance of changes in the dielectric properties of water to the experimentally observed disorder-to-order transition.

Thermodynamic Driving Forces Leading to the Inverse Disorder−Order Transition. In the two-dimensional Ising model, the critical temperature of the transition is dependent on the magnitude of the NN interaction favoring aligned orientations, J, and the number of NNs, z, as $T_c = zJ/2k$ where k is the Boltzmann constant. Our computed free energy differences, proportional to the J values, are similar for the head-in and head-out states. This suggests that as the number of Tag-1 nearest-neighbors z for a Tag-1 is larger in the head-in state, the transition temperature is higher in the head-in state and the free energy bias favoring the aligned state is greater in the head-in state. However, this does not explain the inverted nature of the transition, in which the ordered state is predominant at high temperature.

Our system lacks the symmetry of the 2D Ising model in that the fully aligned head-in and head-out states represent different states of the system, as is observed in the Ising model in an external field. Incorporation of an external field in the Ising model could explain the preference for the head-in state, but not the appearance of the ordered state as the dominant state at high temperatures.

CONCLUSIONS

In this study, we have explored the disorder-to-order transition in the orientational distribution of a modified form of cholesterol (Tag-1). The chemical modification involves replacing the hydroxyl headgroup with an ester group linking a terminal alkyne moiety. The alkyne group provides a unique Raman signature frequency that depends on the surrounding chemical environments. By interpreting the Raman spectra as a function of temperature, the Tag-1 molecule was found to acquire both head-in and head-out orientations indicated by the doublet peak in the Raman spectra in liposomes and lipid-coated noble metal nanoparticles.[32] The signature doublet

https://doi.org/10.1021/jacs.4c09495
J. Am. Chem. Soc. XXXX, XXX, XXX−XXX

peak was observed in both saturated and unsaturated lipid environments in the equilibrium state at room temperature, but undergoes a transition to a singlet peak consistent with an all head-in state at temperatures above 64 °C in the presence of saturated lipids. In contrast, a persistent doublet peak was observed at all temperatures studied in the presence of unsaturated lipids.

We performed molecular dynamics simulations of the lipid bilayer containing 40 mol % Tag-1, 5 mol % DOPS, and 55 mol % DPPC or DOPC. Although both head-in and head-out orientations of Tag-1 were observed in the presence of DPPC and DOPC, the underlying molecular interactions were found to be substantially different. The membrane bilayer was found to form a liquid-ordered phase in the presence of DPPC, in which the populations of both orientations of Tag-1 were found to be stable. No spontaneous flip-flop of Tag-1 was observed. In contrast, in the presence of DOPC the membrane bilayer was observed to form a liquid-disordered phase, in which the head-in and head-out orientations of Tag-1 coexist due to the spontaneous flip-flop of Tag-1.

Tag-1 molecules were found to interact predominantly via the α-face in both ordered and disordered lipid bilayers. In bilayers primarily composed of DPPC, the Tag-1 molecule was stabilized by the favorable interactions between neighboring Tag-1 molecules mediated by the sterol rings. In bilayers primarily composed of DOPC, a energy barrier separating the two different orientations of Tag-1 was observed to be smaller than the barrier for reorientation in the bilayer primarily composed of DPPC, consistent with the spontaneous flip-flop of Tag-1 observed in our simulations and the coexistence of both orientations.

Overall, this study effectively characterizes the orientational dimorphism of a modified form of cholesterol in diverse membrane domains and provides insight into the nature of normal cholesterol interactions in membrane domains predominantly composed of saturated or unsaturated lipids over a wide range of temperatures. Nevertheless, there are key unanswered questions related to the temperature dependence of this transition. Our simulations fail to reproduce the transition to the all head-in state observed in experimental observations at high temperatures. This suggests a shortcoming of the force field that is primarily parametrized for simulations near room temperature. At temperatures exceeding 60 °C, water is a significantly less polar solvent. In principle, this effect may be captured through the use of a polarizable force field. However, at this time we lack a polarizable lipid force field for the set of lipids and cholesterol used in this study, so that must remain a goal for future studies.

METHODS

Computational Models and Methods. We simulated membrane bilayers composed of 55 mol % DPPC/DOPC, 5 mol % DOPS, and 40 mol % Tag-1 (Figure 7 and Supporting Information Figure 1). Each bilayer containing 200 lipids was constructed using Packmol.[50] The bilayers were solvated with 37 water molecules per lipid, defined by the TIP3P water model.[51] 10 K^+ ions were added to neutralize the system charges. Lipids were simulated using the CHARMM36 force field.[52] The force field of Tag-1 was constructed from a predetermined force field of chemical fragments as per CHARMM protocol.[53] Each bilayer was equilibrated for a minimum of 100 ns using the CHARMM-GUI protocol[54] followed by a 1 μs production run was performed. Simulations were performed in the *NPT* ensemble, the leapfrog integration method was used with a 2 fs time step. The electrostatic potential was calculated using particle

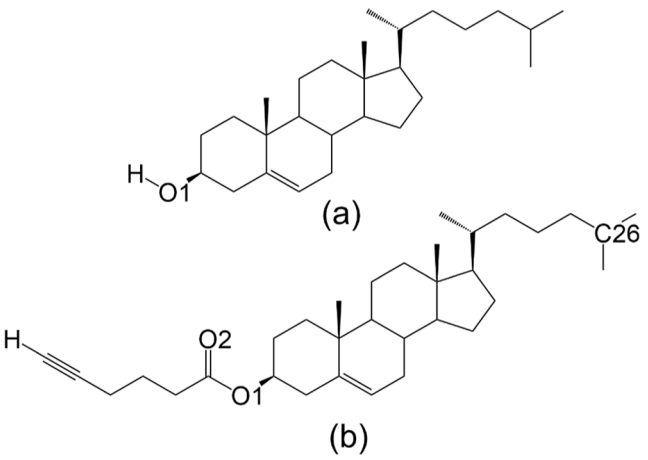

Figure 7. Molecular structures of (a) cholesterol and (b) Tag-1 with atom names used in simulations.

mesh Ewald. The Lennard-Jones potential was calculated using a cutoff of 1.2 nm and a force-switch function over the range 1 to 1.2 nm. A semi-isotropic Parrinello−Rahman barostat was used to maintain the pressure at 1 bar. The temperature of the systems was maintained at 303 K using the Nose−Hoover thermostat. Simulations of the membrane containing C-Laurdan were performed by introducing 2 mol % C-Laurdan into a membrane bilayer (two molecules in each leaflet) containing Tag-1 in a mixed state of head-out and head-in orientations. Independent simulations were performed at temperatures ranging from 295 to 355 K in 5 K increments. A minimum of 250 ns simulation was performed at each temperature. A Berendsen and Parrinello−Rahman barostat were used to maintain a pressure of 1 bar during equilibration and production run, respectively.

Umbrella sampling simulations were performed to calculate the PMF along the collective variable defined by the distance between the Tag-1 headgroup (O1 atom) and the center of the lipid bilayer. In a bilayer containing DPPC, two Tag-1 molecules were moved in opposite directions in an equilibrated membrane bilayer, while maintaining the same number of lipids in both leaflets (Supporting Information Figure 12). This protocol enhances the computational efficiency by generating two equivalent PMFs using the same amount of simulation required to generate one PMF. To ensure proper overlap between adjacent umbrellas along the collective variable, a harmonic restraint potential with a force constant of 1000 kJ mol^{-1} nm^{-2} was evenly placed at 0.15 nm intervals. A 100 to 200 ns simulation was performed for each umbrella window to calculate a PMF. Convergence of the PMF was assessed based on the difference between two similar PMFs obtained from the simulations of Tag-1 flip-flop starting from different leaflets. In a bilayer containing DOPC, one Tag-1 was moved from head-out to head-in orientation. A harmonic restraint potential with a force constant of 1000 kJ mol^{-1} nm^{-2} was evenly placed at 0.15 nm intervals. Convergence of the PMF was determined by comparing the PMF obtained from the full-length simulation with that obtained by discarding the last 20% of simulation data. G_WHAM module was used to remove the impact of the external umbrella bias in all simulations. All simulations were performed using the GROMACS 2018.3 program.[55]

Voronoi tessellation was performed to analyze the number of NNs of Tag-1 monomers and dimers. An atom position for each acyl chain of DPPC (C315 and C215), DOPC (C317 and C217), and DOPS (C317 and C217) was used while performing Voronoi tessellation. Depending on the conformation of the Tag-1, the position of an atom near the tail site (C26 for head-out) or head site (O1 for head-in) was used. The number of NNs was determined by counting the edges of the Voronoi polygon shared with the nearest atoms.

Experimental Methods. *C-Laurdan GP Measurements and Fabrication of Liposomes.* Liposomes were formulated according to the Bangham method with certain adjustments.[56] A lipid mixture

https://doi.org/10.1021/jacs.4c09495
J. Am. Chem. Soc. XXXX, XXX, XXX−XXX

containing DPPC, cholesterol, DOPS, and C-Laurdan or DOPC, cholesterol, DOPS, and C-Laurdan in chloroform with mol %, as specified in the text, was added to a 25 mL round-bottom flask. The total lipid amount was maintained at 1 μmole. Then, the solvent was removed by rotary evaporation (34 °C, 10 min) to obtain a homogeneous and thin lipid film and the samples were dried overnight under vacuum. Multilamellar vesicles (MLVs) were obtained by adding 1 mL of Milli-Q water to this lipid dry film and then sonicated for 5 min using a probe sonicator (120 Sonic Dismembrator, Fisher Scientific, Waltham, MA). Finally, a dispersion of small unilamellar vesicles was obtained by extruding the obtained MLV dispersion 6 times through a calibrated polycarbonate membrane with a pore diameter of 100 nm using the Avanti mini extruder (Avanti Polar Lipids Inc.).

Steady-state fluorescence measurements with C-Laurdan were performed with a spectrofluorometer (HORIBA, Piscataway, NJ) equipped with temperature control, using 1 cm path length quartz cuvettes. C-Laurdan emission spectra (420−510 nm) of liposomes were collected from 25 to 70 °C at an interval of 1 °C with an equilibration time of 0.5 min at each temperature upon excitation at 405 nm. C-Laurdan GP values at different temperatures were calculated using the difference in emission intensities at 440 and 490 nm according to

$$\mathrm{GP} = \frac{I_{440} - I_{490}}{I_{440} + I_{490}}$$

Raman Characterizations of Liposomes. Liposomes containing Tag-1 were prepared following previously established methods.[32] A mixture of 55% DPPC (or DOPC in the case of liposome Tag-1-DOPC), 5% DOPS and 40% Tag-1 solutions in chloroform were rotary evaporated and vacuumed overnight to form a uniform thin film. Afterward, the lipid film was agitated in water through tip sonication to form an aqueous suspension of liposomes. The liposome suspension was prepared or drop-casted on a silicon wafer substrate for in situ and regular Raman measurements. Raman shifts are calibrated by the silica peak at 520.7 cm^{-1}. For regular Raman measurements, ex situ heating was performed on a hot plate with the temperatures set to room temperature, 40, 60, 80, 90, and 100 °C, respectively. For in situ heating, a Peltier element was used to heat the liposome colloid, and the exact temperature of the Peltier element was then calibrated under the same current and power.

■ ASSOCIATED CONTENT

Data Availability Statement

Initial structures of membrane bilayers containing Tag-1, DOPS, and DPPC/DOPC and GROMACS input files used to perform equilibration and production runs, are freely available at: https://github.com/ayan-majumder95/tag-1_2024.

Supporting Information

The Supporting Information is available free of charge at https://pubs.acs.org/doi/10.1021/jacs.4c09495.

(Table 1) Order parameters of lipids; (Figure 1) Molecular structures of lipids; (Figures 2 and 3) Raman spectra analysis; (Figure 4) NN distributions of Tag-1; (Figure 5) Pictorial representation of Tag-1 faces; (Figure 6) Density of DPPC around Tag-1; (Figure 7) Crick angle distribution of Tag-1 dimers; (Figure 8) PMF characterizing Tag-1 orientations in the presence of cholesterols; (Figure 9) Schematic representation of Tag-1 orientations; (Figures 10 and 11) Rotational correlation functions of C-Laurdan; (Figure 12) Schematic representations of the collective variables (PDF)

■ AUTHOR INFORMATION

Corresponding Author

John E. Straub − *Department of Chemistry, Boston University, Boston, Massachusetts 02215, United States;* orcid.org/0000-0002-2355-3316; Email: straub@bu.edu

Authors

Ayan Majumder − *Department of Chemistry, Boston University, Boston, Massachusetts 02215, United States;* orcid.org/0009-0005-4218-3276

Yuanqing Gu − *Department of Chemistry, Boston University, Boston, Massachusetts 02215, United States; The Photonics Center, Boston University, Boston, Massachusetts 02215, United States;* orcid.org/0009-0001-8919-3368

Yi-Chen Chen − *Department of Chemistry, Boston University, Boston, Massachusetts 02215, United States*

Xingda An − *Department of Chemistry, Boston University, Boston, Massachusetts 02215, United States; The Photonics Center, Boston University, Boston, Massachusetts 02215, United States;* orcid.org/0000-0002-7484-7410

Björn M. Reinhard − *Department of Chemistry, Boston University, Boston, Massachusetts 02215, United States; The Photonics Center, Boston University, Boston, Massachusetts 02215, United States;* orcid.org/0000-0003-2550-5331

Complete contact information is available at: https://pubs.acs.org/10.1021/jacs.4c09495

Notes

The authors declare no competing financial interest.

■ ACKNOWLEDGMENTS

The authors gratefully acknowledge the generous support of the National Institutes of Health (grant nos R01 GM107703, R01CA138509, R01AI175068), National Science Foundation (grant no. CHE1900416), and the high-performance computing resources of the Boston University Shared Computing Cluster (SCC). We thank the reviewers for insightful comments that improved the overall quality of our manuscript.

■ REFERENCES

(1) Pinkwart, K.; Schneider, F.; Lukoseviciute, M.; Sauka-Spengler, T.; Lyman, E.; Eggeling, C.; Sezgin, E. Nanoscale Dynamics of Cholesterol in the Cell Membrane. *J. Biol. Chem.* **2019**, *294* (34), 12599−12609.

(2) Van Meer, G.; Voelker, D. R.; Feigenson, G. W. Membrane Lipids: Where They Are and How They Behave. *Nat. Rev. Mol. Cell Biol.* **2008**, *9* (2), 112−124.

(3) Fantini, J.; Barrantes, F. J. How Cholesterol Interacts with Membrane Proteins: An Exploration of Cholesterol-Binding Sites Including CRAC, CARC, and Tilted Domains. *Front. Physiol.* **2013**, *4*, 31.

(4) Ohvo-Rekilä, H.; Ramstedt, B.; Leppimäki, P.; Peter Slotte, J. Cholesterol Interactions with Phospholipids in Membranes. *Prog. Lipid Res.* **2002**, *41* (1), 66−97.

(5) Martin, R. B.; Yeagle, P. L. Models for Lipid Organization in Cholesterol-Phospholipid Bilayers Including Cholesterol Dimer Formation. *Lipids* **1978**, *13* (9), 594−597.

(6) Song, Y.; Kenworthy, A. K.; Sanders, C. R. Cholesterol as a Co-Solvent and a Ligand for Membrane Proteins. *Protein Sci.* **2014**, *23* (1), 1−22.

(7) Ohvo-Rekilä, H.; Ramstedt, B.; Leppimäki, P.; Peter Slotte, J. Cholesterol Interactions with Phospholipids in Membranes. *Prog. Lipid Res.* **2002**, *41* (1), 66−97.

(8) Saher, G.; Brügger, B.; Lappe-Siefke, C.; Möbius, W.; Tozawa, R. I.; Wehr, M. C.; Wieland, F.; Ishibashi, S.; Nave, K. A. High

Cholesterol Level Is Essential for Myelin Membrane Growth. *Nat. Neurosci.* **2005**, *8* (4), 468−475.
(9) Pantelopulos, G. A.; Nagai, T.; Bandara, A.; Panahi, A.; Straub, J. E. Critical Size Dependence of Domain Formation Observed in Coarse-Grained Simulations of Bilayers Composed of Ternary Lipid Mixtures. *J. Chem. Phys.* **2017**, *147* (9), 095101.
(10) Bandara, A.; Panahi, A.; Pantelopulos, G. A.; Nagai, T.; Straub, J. E. Exploring the Impact of Proteins on the Line Tension of a Phase-Separating Ternary Lipid Mixture. *J. Chem. Phys.* **2019**, *150* (20), 204702.
(11) Reitz, C. Alzheimer's Disease and the Amyloid Cascade Hypothesis: A Critical Review. *Int. J. Alzheimer's Dis.* **2012**, *2012*, 1−11.
(12) Simons, K.; Ehehalt, R. Cholesterol, Lipid Rafts, and Disease. *J. Clin. Invest.* **2002**, *110* (5), 597−603.
(13) Kobayashi, T.; Menon, A. K. Transbilayer Lipid Asymmetry. *Curr. Biol.* **2018**, *28* (8), R386−R391.
(14) Ikeda, M.; Kihara, A.; Igarashi, Y. Lipid Asymmetry of the Eukaryotic Plasma Membrane: Functions and Related Enzymes. *Biol. Pharm. Bull.* **2006**, *29* (8), 1542−1546.
(15) Contreras, F.-X.; Sánchez-Magraner, L.; Alonso, A.; Goñi, F. M. Transbilayer (Flip-Flop) Lipid Motion and Lipid Scrambling in Membranes. *FEBS Lett.* **2010**, *584* (9), 1779−1786.
(16) Van Meer, G.; Voelker, D. R.; Feigenson, G. W. Membrane Lipids: Where They Are and How They Behave. *Nat. Rev. Mol. Cell Biol.* **2008**, *9* (2), 112−124.
(17) Zachowski, A.; Devaux, P. F. Transmembrane Movements of Lipids. *Experientia* **1990**, *46* (6), 644−656.
(18) de Kruijff, B.; van den Besselaar, A. M. H. P.; Cullis, P. R.; van den Bosch, H.; van Deenen, L. L. M. Evidence for Isotropic Motion of Phospholipids in Liver Microsomal Membranes. A 31P NMR Study. *Biochim. Biophys. Acta, Biomembr.* **1978**, *514* (1), 1−8.
(19) Leventis, R.; Silvius, J. R. Use of Cyclodextrins to Monitor Transbilayer Movement and Differential Lipid Affinities of Cholesterol. *Biophys. J.* **2001**, *81* (4), 2257−2267.
(20) Garg, S.; Porcar, L.; Woodka, A. C.; Butler, P. D.; Perez-Salas, U. Noninvasive Neutron Scattering Measurements Reveal Slower Cholesterol Transport in Model Lipid Membranes. *Biophys. J.* **2011**, *101* (2), 370−377.
(21) Bruckner, R. J.; Mansy, S. S.; Ricardo, A.; Mahadevan, L.; Szostak, J. W. Flip-Flop-Induced Relaxation of Bending Energy: Implications for Membrane Remodeling. *Biophys. J.* **2009**, *97* (12), 3113−3122.
(22) Bennett, W. F. D.; MacCallum, J. L.; Hinner, M. J.; Marrink, S. J.; Tieleman, D. P. Molecular View of Cholesterol Flip-Flop and Chemical Potential in Different Membrane Environments. *J. Am. Chem. Soc.* **2009**, *131* (35), 12714−12720.
(23) Bacia, K.; Schwille, P.; Kurzchalia, T. Sterol Structure Determines the Separation of Phases and the Curvature of the Liquid-Ordered Phase in Model Membranes. *Proc. Natl. Acad. Sci. U.S.A.* **2005**, *102* (9), 3272−3277.
(24) Yu, T.; Zhou, G.; Hu, X.; Ye, S. Transport and Organization of Cholesterol in a Planar Solid-Supported Lipid Bilayer Depend on the Phospholipid Flip-Flop Rate. *Langmuir* **2016**, *32* (44), 11681−11689.
(25) Steck, T. L.; Ye, J.; Lange, Y. Probing Red Cell Membrane Cholesterol Movement with Cyclodextrin. *Biophys. J.* **2002**, *83* (4), 2118−2125.
(26) Jo, S.; Rui, H.; Lim, J. B.; Klauda, J. B.; Im, W. Cholesterol Flip-Flop: Insights from Free Energy Simulation Studies. *J. Phys. Chem. B* **2010**, *114* (42), 13342−13348.
(27) Choubey, A.; Kalia, R. K.; Malmstadt, N.; Nakano, A.; Vashishta, P. Cholesterol Translocation in a Phospholipid Membrane. *Biophys. J.* **2013**, *104* (11), 2429−2436.
(28) Parisio, G.; Ferrarini, A.; Sperotto, M. M. Model Studies of Lipid Flip-Flop in Membranes. *Int. J. Adv. Eng. Sci. Appl. Math.* **2016**, *8* (2), 134−146.
(29) Parisio, G.; Sperotto, M. M.; Ferrarini, A. Flip-Flop of Steroids in Phospholipid Bilayers: Effects of the Chemical Structure on Transbilayer Diffusion. *J. Am. Chem. Soc.* **2012**, *134* (29), 12198−12208.
(30) Bennett, W. F. D.; Tieleman, D. P. Molecular Simulation of Rapid Translocation of Cholesterol, Diacylglycerol, and Ceramide in Model Raft and Nonraft Membranes. *J. Lipid Res.* **2012**, *53* (3), 421−429.
(31) Marrink, S. J.; de Vries, A. H.; Harroun, T. A.; Katsaras, J.; Wassall, S. R. Cholesterol Shows Preference for the Interior of Polyunsaturated Lipid Membranes. *J. Am. Chem. Soc.* **2008**, *130* (1), 10−11.
(32) An, X.; Majumder, A.; McNeely, J.; Yang, J.; Puri, T.; He, Z.; Liang, T.; Snyder, J. K.; Straub, J. E.; Reinhard, B. M. Interfacial Hydration Determines Orientational and Functional Dimorphism of Sterol-Derived Raman Tags in Lipid-Coated Nanoparticles. *Proc. Natl. Acad. Sci. U.S.A.* **2021**, *118* (33), No. e2105913118.
(33) Pantelopulos, G. A.; Straub, J. E. Regimes of Complex Lipid Bilayer Phases Induced by Cholesterol Concentration in MD Simulation. *Biophys. J.* **2018**, *115* (11), 2167−2178.
(34) Uppamoochikkal, P.; Tristram-Nagle, S.; Nagle, J. F. Orientation of Tie-Lines in the Phase Diagram of DOPC/DPPC/Cholesterol Model Biomembranes. *Langmuir* **2010**, *26* (22), 17363−17368.
(35) Wang, Y.; Gkeka, P.; Fuchs, J. E.; Liedl, K. R.; Cournia, Z. DPPC-Cholesterol Phase Diagram Using Coarse-Grained Molecular Dynamics Simulations. *Biochim. Biophys. Acta, Biomembr.* **2016**, *1858* (11), 2846−2857.
(36) Majumder, A.; Vuksanovic, N.; Ray, L. C.; Bernstein, H. M.; Allen, K. N.; Imperiali, B.; Straub, J. E. Synergistic Computational and Experimental Studies of a Phosphoglycosyl Transferase Membrane/Ligand Ensemble. *J. Biol. Chem.* **2023**, *299* (10), 105194.
(37) Engelman, D. M.; Rothman, J. E. The Planar Organization of Lecithin-Cholesterol Bilayers. *J. Biol. Chem.* **1972**, *247* (11), 3694−3697.
(38) Bandara, A.; Panahi, A.; Pantelopulos, G. A.; Straub, J. E. Exploring the Structure and Stability of Cholesterol Dimer Formation in Multicomponent Lipid Bilayers. *J. Comput. Chem.* **2017**, *38* (16), 1479−1488.
(39) Kulig, W.; Mikkolainen, H.; Olżyńska, A.; Jurkiewicz, P.; Cwiklik, L.; Hof, M.; Vattulainen, I.; Jungwirth, P.; Rog, T. Bobbing of Oxysterols: Molecular Mechanism for Translocation of Tail-Oxidized Sterols through Biological Membranes. *J. Phys. Chem. Lett.* **2018**, *9* (5), 1118−1123.
(40) Osella, S.; Murugan, N. A.; Jena, N. K.; Knippenberg, S. Investigation into Biological Environments through (Non)Linear Optics: A Multiscale Study of Laurdan Derivatives. *J. Chem. Theory Comput.* **2016**, *12* (12), 6169−6181.
(41) Kim, H. M.; Choo, H. J.; Jung, S. Y.; Ko, Y. G.; Park, W. H.; Jeon, S. J.; Kim, C. H.; Joo, T.; Cho, B. R.; Cho, B. R. A Two-Photon Fluorescent Probe for Lipid Raft Imaging: C-Laurdan. *ChemBioChem* **2007**, *8*, 553−559.
(42) Harris, F. M.; Best, K. B.; Bell, J. D. Use of Laurdan Fluorescence Intensity and Polarization to Distinguish between Changes in Membrane Fluidity and Phospholipid Order. *Biochim. Biophys. Acta* **2002**, *1565*, 123−128.
(43) Lipari, G.; Szabo, A. Effect of Librational Motion on Fluorescence Depolarization and Nuclear Magnetic Resonance Relaxation in Macromolecules and Membranes. *Biophys. J.* **1980**, *30* (3), 489−506.
(44) Kinosita, K.; Kawato, S.; Ikegami, A. A Theory of Fluorescence Polarization Decay in Membranes. *Biophys. J.* **1977**, *20* (3), 289−305.
(45) Gu, Y.; Reinhard, B. M. Membrane Fluidity Properties of Lipid-Coated Polylactic Acid Nanoparticles. *Nanoscale* **2024**, *16*, 8533−8545.
(46) Chiang, Y.-W.; Costa-Filho, A. J.; Freed, J. H. Dynamic Molecular Structure and Phase Diagram of DPPC-Cholesterol Binary Mixtures: A 2D-ELDOR Study. *J. Phys. Chem. B* **2007**, *111* (38), 11260−11270.
(47) Vist, M. R.; Davis, J. H. Phase equilibria of cholesterol/dipalmitoylphosphatidylcholine mixtures: deuterium nuclear magnetic

https://doi.org/10.1021/jacs.4c09495
J. Am. Chem. Soc. XXXX, XXX, XXX−XXX

resonance and differential scanning calorimetry. *Biochemistry* **1990**, *29* (2), 451−464.
(48) Nyholm, T. K. M.; Lindroos, D.; Westerlund, B.; Slotte, J. P. Construction of a DOPC/PSM/Cholesterol Phase Diagram Based on the Fluorescence Properties of Trans -Parinaric Acid. *Langmuir* **2011**, *27* (13), 8339−8350.
(49) Konyakhina, T. M.; Wu, J.; Mastroianni, J. D.; Heberle, F. A.; Feigenson, G. W. Phase Diagram of a 4-Component Lipid Mixture: DSPC/DOPC/POPC/Chol. *Biochim. Biophys. Acta, Biomembr.* **2013**, *1828* (9), 2204−2214.
(50) Martínez, L.; Andrade, R.; Birgin, E. G.; Martínez, J. M. PACKMOL: A Package for Building Initial Configurations for Molecular Dynamics Simulations. *J. Comput. Chem.* **2009**, *30* (13), 2157−2164.
(51) Jorgensen, W. L.; Chandrasekhar, J.; Madura, J. D.; Impey, R. W.; Klein, M. L. Comparison of Simple Potential Functions for Simulating Liquid Water. *J. Chem. Phys.* **1983**, *79* (2), 926−935.
(52) Klauda, J. B.; Venable, R. M.; Freites, J. A.; O'Connor, J. W.; Tobias, D. J.; Mondragon-Ramirez, C.; Vorobyov, I.; MacKerell, A. D.; Pastor, R. W. Update of the CHARMM All-Atom Additive Force Field for Lipids: Validation on Six Lipid Types. *J. Phys. Chem. B* **2010**, *114* (23), 7830−7843.
(53) Vanommeslaeghe, K.; Hatcher, E.; Acharya, C.; Kundu, S.; Zhong, S.; Shim, J.; Darian, E.; Guvench, O.; Lopes, P.; Vorobyov, I.; Mackerell, A. D. CHARMM General Force Field: A Force Field for Drug-like Molecules Compatible with the CHARMM All-Atom Additive Biological Force Fields. *J. Comput. Chem.* **2010**, *31* (4), 671−690.
(54) Jo, S.; Cheng, X.; Lee, J.; Kim, S.; Park, S. J.; Patel, D. S.; Beaven, A. H.; LeeRuiPark, K. H. S.; Lee, H. S.; Roux, B.; MacKerell, A. D.; Klauda, J. B.; Qi, Y.; Im, W.; Qi, Y.; Im, W. CHARMM-GUI 10 Years for Biomolecular Modeling and Simulation. *J. Comput. Chem.* **2017**, *38* (15), 1114−1124.
(55) Abraham, M. J.; Murtola, T.; Schulz, R.; Páll, S.; Smith, J. C.; Hess, B.; Lindahl, E. GROMACS: High Performance Molecular Simulations through Multi-Level Parallelism from Laptops to Supercomputers. *SoftwareX* **2015**, *1*−*2*, 19−25.
(56) Bangham, A. D.; Standish, M. M.; Watkins, J. C. Diffusion of Univalent Ions across the Lamellae of Swollen Phospholipids. *J. Mol. Biol.* **1965**, *13* (1), 238.

https://doi.org/10.1021/jacs.4c09495
J. Am. Chem. Soc. XXXX, XXX, XXX−XXX